



This is a repository copy of *Three-dimensional millimetre wave beam tracking based on handset MEMS sensors with extended Kalman filtering*.

White Rose Research Online URL for this paper:  
<http://eprints.whiterose.ac.uk/110820/>

Version: Accepted Version

---

**Proceedings Paper:**

Qi, Z. and Liu, W. [orcid.org/0000-0003-2968-2888](https://orcid.org/0000-0003-2968-2888) (2016) Three-dimensional millimetre wave beam tracking based on handset MEMS sensors with extended Kalman filtering. In: Radio Propagation and Technologies for 5G. Radio Propagation and Technologies for 5G, 03/06/2016, Durham, UK. IET . ISBN 978-1-78561-401-9

<https://doi.org/10.1049/ic.2016.0066>

---

**Reuse**

Unless indicated otherwise, fulltext items are protected by copyright with all rights reserved. The copyright exception in section 29 of the Copyright, Designs and Patents Act 1988 allows the making of a single copy solely for the purpose of non-commercial research or private study within the limits of fair dealing. The publisher or other rights-holder may allow further reproduction and re-use of this version - refer to the White Rose Research Online record for this item. Where records identify the publisher as the copyright holder, users can verify any specific terms of use on the publisher's website.

**Takedown**

If you consider content in White Rose Research Online to be in breach of UK law, please notify us by emailing [eprints@whiterose.ac.uk](mailto:eprints@whiterose.ac.uk) including the URL of the record and the reason for the withdrawal request.



[eprints@whiterose.ac.uk](mailto:eprints@whiterose.ac.uk)  
<https://eprints.whiterose.ac.uk/>

# Three-Dimensional Millimetre Wave Beam Tracking Based on Handset MEMS Sensors with Extended Kalman Filtering

Zichen Qi and Wei Liu

Communications Research Group, Department of Electronic and Electrical Engineering  
University of Sheffield, Sheffield S1 3JD, United Kingdom  
{zqi2, w.liu}@sheffield.ac.uk

**Keywords:** MEMS sensor, three-dimensional tracking, beam steering, millimeter wave communication, extended Kalman filtering

*Abstract*—Due to the narrow beam in millimetre wave communication for future 5G networks, small device movements in the form of either self-rotation or displacement can result in serious power loss. In this paper, a three-dimensional (3-D) beam tracking method employing extended Kalman filtering (EKF) is proposed based on antenna arrays and the three smart phone sensors, which are gyroscope, accelerometer and magnetometer, embedded in the micro-electro-mechanical system (MEMS) inside the smart phone. The EKF-based location tracking is also incorporated into the design by combing the data from direction of arrival (DoA) and time of arrival (ToA) estimation results of the user node (UN), since accurate UN location information is also very important in the process of beam tracking to achieve beam alignment between the access node (AN) and the UN.

## I. INTRODUCTION

In 5G ultra dense networks, it is envisaged that the distance between different access nodes (ANs) and user nodes (UNs) would be in the range of tens of meters or even less. As a result, UNs are mainly in the line of sight (LoS) communication with ANs [1]. However, due to the inherent property of millimetre wave for transmission and reception, the beam alignment between the AN and the UN can be easily destroyed by even a slight movement of the UN, causing significant loss in the received signal power. Therefore, the user's behavioral (self-rotation) and location information is essential to maintain an acceptable level of communication link between the AN and the UN.

However, traditional commercial positioning techniques cannot meet the requirements of 5G beam tracking, including the global navigation satellite systems (GNSSs) with a root mean square error (RMSE) of 5m [2], LTE observed time difference of arrival (OTDoA) with an RMSE of about 25m [3], and WLAN fingerprinting of about 3m to 4m [4]. Fortunately, the extremely short wavelength of millimeter wave

renders installation of a large number of array antennas at both UNs and ANs possible and the wide bandwidth can lead to highly accurate position measurements such as ToA (time of arrival) and TDoA (time difference of arrival). In [5], a joint DoA/ToA tracking method based on extended Kalman filtering (EKF) and a clock offset positioning method was proposed with an accuracy of about 0.1m. By combining DoA and RSS (received signal strength), a low-complexity localization system was presented in [6]. Furthermore, the angle information acquired from DoA is applied in direction lock loop for tracking purposes in [7].

On the other hand, for 5G millimetre wave beam tracking, only a few research results have been reported in literature. In [8], a method for tracking the signal to noise ratio (SNR) of the channel with prediction and detection was proposed. In [9], the effect of circular motion of the devices at 60GHz was studied. The experimental results of beam tracking for the base station in an indoor environment was presented in [10]. Moreover, a Kalman filter based beam tracking method with mobile sensors was introduced in [11].

In this paper, as further extension of the work in [11], a three-dimensional (3-D) tracking method is proposed to maintain the beam alignment between AN and UN in the 5G network using sensors embedded in smart phones. The considered scenario is a single user in an ultra-dense network with an LOS communication link. Compared to the work in [11], we incorporate UN location tracking into the design and consider 3-D tracking with quaternion-valued rotation modelling. More specifically, a combination of DoA and ToA with extended Kalman filter is used for location tracking; a uniform rectangular array is employed at the UN for 3-D beamforming and its main beam is adjusted towards the signal direction whenever it is below a preset threshold value; beam steering is employed for better performance instead of the fixed beam switching scheme adopted in [11]. For tracking behavioral changes (self-rotation) of the UN, we use the IMU (inertial measurement unit) of the smart phone to give self-

measurements of the moving device. An IMU includes a three-axis gyroscope (for measurement of angular velocity), a three-axis accelerometer (for acceleration measurement), and a three-axis magnetometer (for magnetic field measurement), which are embedded in the micro-electro-mechanical system (MEMS) inside the smart phone. The data obtained from these sensors are incorporated by EKF for tracking behavioral changes of the UN, where the gyroscope gives state update, while accelerometer and magnetometer give measurement update to correct the gyroscope drift error.

This paper is organized as follows. Models of the coordinate system and the three embedded sensors in the smart phone, and the proposed 3-D rotation tracking method are presented in Sec. II. Simulation results are provided in Sec. III and conclusions are drawn in Sec. IV.

## II. SELF-ROTATION TRACKING

### A. Euler Angles and Coordinate Transform

The popular rotation angle set of yaw( $\gamma$ )-pitch( $\beta$ )-roll( $\alpha$ ) (also expressed in z-y-x form) is chosen and rotation can be expressed as a sequence with initial status  $z_0 - y_0 - x_0$ , first rotation  $z_1 - y_1 - x_1$ , second rotation  $z_2 - y_2 - x_2$  and final rotation  $z_3 - y_3 - x_3$ . The three rotation processes can be represented individually in the form of the Direction Cosine Matrix (DCM) as three basic clockwise rotations.

A yaw rotation around z-axis is defined as

$$\mathbf{R}_z(\gamma) = \begin{bmatrix} \cos \gamma & -\sin \gamma & 0 \\ \sin \gamma & \cos \gamma & 0 \\ 0 & 0 & 1 \end{bmatrix}. \quad (1)$$

A pitch rotation around y-axis is defined as

$$\mathbf{R}_y(\beta) = \begin{bmatrix} \cos \beta & 0 & \sin \beta \\ 0 & 1 & 0 \\ -\sin \beta & 0 & \cos \beta \end{bmatrix}. \quad (2)$$

A roll rotation around x-axis is defined as

$$\mathbf{R}_x(\alpha) = \begin{bmatrix} 1 & 0 & 0 \\ 0 & \cos \alpha & -\sin \alpha \\ 0 & \sin \alpha & \cos \alpha \end{bmatrix}. \quad (3)$$

A combination of the three DCMs is often called the rotation matrix:

$$\mathbf{R} = \begin{bmatrix} \cos \beta \cos \gamma & & & \\ \sin \alpha \sin \beta \cos \gamma - \cos \alpha \sin \beta & & & \\ \cos \alpha \sin \beta \cos \gamma + \sin \alpha \sin \beta & & & \\ & \cos \beta \sin \gamma & -\sin \beta & \\ & \sin \alpha \sin \beta \sin \gamma + \cos \alpha \cos \gamma & \sin \alpha \cos \beta & \\ & \cos \alpha \sin \beta \sin \gamma - \sin \alpha \cos \gamma & \cos \alpha \cos \beta & \end{bmatrix} \quad (4)$$

$K$  ANs are considered in an ultra-dense network for UN positioning. The location  $P_{a,k} = (x_{a,k}, y_{a,k}, z_{a,k})$  of each

AN defined in north-east-down (NED) local-level frame (LLF) is assumed to be known in advance with  $k = 1, 2, \dots, K$ . In the process of position tracking using EKF [12], the UN sends a pilot signal periodically to communicate with the ANs. Thereafter, measurements from ToA and DoA are gathered by the network to yield a UN position estimate.

The location information of the UN  $P_{u,k} = (x_{u,k}, y_{u,k}, z_{u,k})$ ,  $k = 1, 2, \dots, K$ , is also defined in NED. Thus, the line of sight vector is calculated as

$$\mathbf{l}_l = P_{u,k} - P_{a,k} \quad (5)$$

so  $\mathbf{l}_l = [x_{u,k} - x_{a,k} \quad y_{u,k} - y_{a,k} \quad z_{u,k} - z_{a,k}]^T$  and the LoS vector can be expressed with the Euler angle as

$$\mathbf{l}_b = \mathbf{R}_l^b \mathbf{l}_l. \quad (6)$$

### B. Sensor Signal Modelling

There are three sensors embedded in a smart phone: a three-axis gyroscope, a three-axis accelerometer and a three-axis magnetometer. Although the gyroscope itself can measure the three rotation angles (yaw, pitch, roll) accurately in short time, the drift error caused by integration could cause significant errors in rotation tracking [13]. Besides, neither magnetometer nor accelerometer can give reliable measurements. As a result, measurements from the three sensors have to be combined by EKF to achieve a relatively high accuracy in rotation angle tracking.

The output of the gyroscope is angular velocity. It can be expressed as follows

$$\boldsymbol{\omega}_b = \begin{bmatrix} \omega_x \\ \omega_y \\ \omega_z \end{bmatrix} \quad (7)$$

Thus, the gyroscope data can be modelled as

$$\mathbf{y}_g = \boldsymbol{\omega}_b + \mathbf{b}_g + \mathbf{n}_g, \quad (8)$$

where  $\mathbf{y}_g$  is the angular velocity measured from gyroscope,  $\mathbf{b}_g$  is the bias of gyroscope or the drift error, and  $\mathbf{n}_g$  is zero-mean white Gaussian noise.

The three-axis accelerometer measures the acceleration of each axis and transform the data into roll and pitch angles. The yaw angle (rotation around the z-axis) cannot be determined from the accelerometer [13]. The problem of accelerometer is mainly caused by additional force placed on the handset and gravity needs to be subtracted from the model.

The output of the accelerometer and the transformation to rotation angle are given by:

$$\mathbf{y}_a = \mathbf{a}_a + \mathbf{b}_a + \mathbf{n}_a \quad (9)$$

$$\mathbf{a}_a = [a_x \quad a_y \quad a_z - g]^T \quad (10)$$

$$\alpha_{acc} = \text{atan2}(-y_{a,y}, -y_{a,z}) \quad (11)$$

$$\beta_{acc} = \text{atan2}(-y_{a,x}, \sqrt{y_{a,y}^2 + y_{a,z}^2}) \quad (12)$$

where  $\mathbf{y}_a$  is the acceleration measured from the accelerometer,  $\mathbf{b}_a$  is the bias, which follows the Gauss-Markov model [14],  $\mathbf{n}_a$  is zero-mean white Gaussian noise,  $\alpha_{acc}$  and  $\beta_{acc}$  are the roll and pitch angles calculated from the accelerometer,  $g$  is the earth's gravity, and  $\text{atan2}$  is a four-quadrant inverse tangent function [15]:

$$\text{atan2}(y, x) = \begin{cases} \arccatan\frac{y}{x} & \text{if } x > 0, \\ \frac{\pi}{2} - \arccatan\frac{x}{y} & \text{if } y > 0, \\ -\frac{\pi}{2} - \arccatan\frac{x}{y} & \text{if } y < 0, \\ -\arccatan\frac{y}{x} + / - \pi & \text{if } x < 0, \\ \text{undefined} & \text{if } x \text{ and } y = 0, \end{cases} \quad (13)$$

The magnetometer measures the magnetic field. Thus, the yaw angle can be measured from the output data. However, the magnetometer can be easily affected by other magnetic field [13]. So its output and the calculation of yaw angle can be described as

$$\mathbf{y}_m = \mathbf{b}_m + \mathbf{n}_m \quad (14)$$

$$\mathbf{b}_m = [b_x \quad b_y \quad b_z]^T \quad (15)$$

$$\gamma_{mag} = \text{atan2}(-y_{m,y}, y_{m,x}) \quad (16)$$

where  $y_m$  is the data from the magnetometer,  $\gamma_{mag}$  is the calculated yaw angle, and  $\mathbf{n}_m$  is also zero-mean white Gaussian noise.

### C. Tracking Algorithm for Self-Rotation

In smart phone programming, quaternion is a frequently used tool for defining orientation. A quaternion has one real part and three imaginary parts and is noncommutative [16]. In the context of rotation, it is defined with the rotation angle  $\alpha$  by

$$\vec{\mathbf{q}} = \begin{bmatrix} q_0 \\ q_1 \\ q_2 \\ q_3 \end{bmatrix} = \begin{bmatrix} \cos(\frac{\alpha}{2}) \\ x^* \sin(\frac{\alpha}{2}) \\ y^* \sin(\frac{\alpha}{2}) \\ z^* \sin(\frac{\alpha}{2}) \end{bmatrix} \quad (17)$$

The rotation sequence z-y-x can also be expressed in the form of a quaternion as follows

$$\vec{\mathbf{q}} = \begin{bmatrix} \gamma \\ \beta \\ \alpha \end{bmatrix} = \begin{bmatrix} \text{atan2}(2q_2q_3 + 2q_0q_1, q_3^2 - q_2^2 - q_1^2 + q_0^2) \\ -\text{asin}(2q_1q_3 - 2q_0q_2) \\ \text{atan2}(2q_1q_2 + 2q_0q_3, q_1^2 + q_0^2 - q_3^2 + q_2^2) \end{bmatrix} \quad (18)$$

Based on the quaternion method, we can calculate the Euler angle with the data from the gyroscope by

$$\dot{\mathbf{q}}_g[i] = \frac{d\mathbf{q}_g[i]}{dt} = \frac{1}{2} * \mathbf{q}_g[i-1] \otimes \mathbf{y}_g \quad (19)$$

$$\mathbf{q}_g[i] = \mathbf{q}_g[i-1] + \Delta_t * \frac{d\mathbf{q}_g[i]}{dt} \quad (20)$$

where  $\dot{\mathbf{q}}_g[i]$  is the quaternion rate.

The tracking of rotation is conducted by combining the data from the three sensors using the EKF algorithm. In detail, the data from the gyroscope is set as the estimated value and the data from the accelerometer and the magnetometer is the measurement result. The state vector equations are shown as follows with  $q_m[i]$  denoting the quaternion-valued measurement vector

$$\dot{\mathbf{q}}_g[i] = \begin{bmatrix} \dot{q}_{g,1}[i] \\ \dot{q}_{g,2}[i] \\ \dot{q}_{g,3}[i] \\ \dot{q}_{g,4}[i] \end{bmatrix} = \frac{1}{2} \begin{bmatrix} q_{g,1}[i] \\ q_{g,2}[i] \\ q_{g,3}[i] \\ q_{g,4}[i] \end{bmatrix} \otimes \begin{bmatrix} 0 \\ y_{g,x} \\ y_{g,y} \\ y_{g,z} \end{bmatrix} \quad (21)$$

$$\mathbf{q}_m[i] = \begin{bmatrix} q_{m,1}[i] \\ q_{m,2}[i] \\ q_{m,3}[i] \\ q_{m,4}[i] \end{bmatrix} = \begin{bmatrix} 0 \\ \gamma_{mag} \\ \beta_{acc} \\ \alpha_{acc} \end{bmatrix} \quad (22)$$

The state vector of a UN's rotation angle obtained from the gyroscope is defined as  $\mathbf{s}[i] = \vec{\mathbf{q}}_g[i]$  which evolves from the dynamic model below, with  $\vec{\mathbf{q}}_g[i]$  indicating the gyroscope output without measurement noise,

$$\mathbf{s}[i] = f(\mathbf{s}[i-1]) + \mathbf{w}[i] \quad (23)$$

where  $\mathbf{s}[i]$  consists of the UN's rotation angle state in time index  $i$ , which is changing following the function  $f(\cdot)$ , with a standard deviation  $\sigma_s$ , and  $\mathbf{w}[i]$  represents the state noise matrix modelled as zero mean white Gaussian with covariance matrix  $\mathbf{Q}$ .

The measurement equation is  $\mathbf{y}[i] = \vec{\mathbf{q}}_m[i] + \mathbf{e}[i]$  with measurement error  $\mathbf{e}[i]$  being zero mean white Gaussian with covariance matrix  $\mathbf{R}$  and  $\vec{\mathbf{q}}_m[i]$  is the measurement output from the accelerometer and the magnetometer without noise. Hence, the measurement vector can be expressed as

$$\mathbf{y}[i] = h(\mathbf{s}[i]) + \mathbf{e}[i]. \quad (24)$$

where  $h(\cdot)$  is the handling function.

The estimation process can then be described as follows

$$\hat{\mathbf{s}}^- [i] = f(\hat{\mathbf{s}}^+ [i-1]) \quad (25)$$

$$\mathbf{P}^- [i] = \mathbf{A}\mathbf{P}^+ [i]\mathbf{A}^T + \mathbf{Q}[i] \quad (26)$$

where (25) represents state prediction,  $\mathbf{s}^+ [i-1]$  is the a priori state, and  $\mathbf{s}^- [i]$  is the posteriori estimate. Likewise,  $\mathbf{P}$  is the covariance matrix representing errors in the estimation process.

The update process with new measurement is given by

$$\mathbf{K}[i] = \frac{\mathbf{P}^- [i]\mathbf{H}[i]}{\mathbf{H}[i]\mathbf{P}^- [i]\mathbf{H}^T [i] + \mathbf{R}[i]} \quad (27)$$

$$\hat{\mathbf{s}}^+ [i] = \hat{\mathbf{s}}^- [i] + \mathbf{K}[i](\mathbf{Y}[i] - \mathbf{H}h(\hat{\mathbf{s}}^- [i])) \quad (28)$$

$$\mathbf{P}^+ [i] = (\mathbf{I} - \mathbf{K}[i]\mathbf{H}[i])\mathbf{P}^- [i] \quad (29)$$

$\mathbf{K}$  is the Kalman gain and  $\mathbf{I}$  is the identity matrix. In equations (26)-(29),  $\mathbf{H}$  and  $\mathbf{A}$  are obtained from Jacobian matrices.

$$\mathbf{A}[i] = \frac{\partial f[i]}{\partial s[i]} \quad (30)$$

$$\mathbf{H}[i] = \frac{\partial h[i]}{\partial s[i]} \quad (31)$$

Finally, the estimated rotation angle of the handset is obtained as  $s^+[i] = \bar{q}^+[i]$  with the update process covariance matrix  $\mathbf{P}^+$ .

### III. SIMULATION AND ANALYSIS

Two scenarios are considered in our simulations: one is self-rotation with a fixed UN position, and the other is self-rotation with short-distance movement of the UN. A  $11 \times 11$  uniform rectangular array with Hamming weight is employed at the UN for 3-D beamforming [17].

In the first scenario, the UN stands at a fixed position with a constant self-rotation speed of  $0.01^\circ$  per ms in all three directions and the operation time is 10s. The delay of sensor measurements can be ignored as it is at the order of nanoseconds. The delay of beam steering is picoseconds and can be ignored too [18]. The accelerometer and magnetometer's measurement noise is set to be  $e_a \sim N(0, \sigma_{e_a}^2)$  with  $\sigma_{e_a} = 1.3m/s$  and  $e_m \sim N(0, \sigma_{e_m}^2)$  with  $\sigma_{e_m} = 1.3ut$ , respectively. The threshold for steering is set to be -2dB of the maximum signal power.

The location tracking EKF employed here is the same as that in the angle tracking with different state and measurement vectors, which are initialized with a coarse estimate obtained from GPS, DoA or some other commercial position systems, since the initial coarse value has little impact on the following tracking process [12]. The update period is  $T_t = 167.3\mu s$  [19]. Within the update cycle, standard deviation (STD) of speed in the state vector  $s_l[i]$  is set to be  $\sigma_{sl} = [0.01m/s, 0.01m/s, 0.01m/s]^T$  with the speed modelled as Gaussian distributed with zero mean and the noise variance from measurement vector  $y_l[i]$  obtained from DoA and ToA is  $\sigma_{el} = 0.6m/s$ . For more details of the location tracking process employed here, please refer to reference [5]. The update process follows the equations from (25) to (29). The operation time is 10s. The tracking result for the first  $167.3ms$  is shown in Fig. 1, with  $n$  being the update index number. We can see that the location of UN is estimated at around (10,1,-10) and the calculated RMSE is 0.5585.

The location information of UN is used in the following beam tracking process and the beam tracking results are presented in Figs. 2-4 for the three rotation angles. We can see that for the case without tracking, the signal power has dropped to a very low level destroying the communication link entirely. In contrast, the sensor-aided tracking method

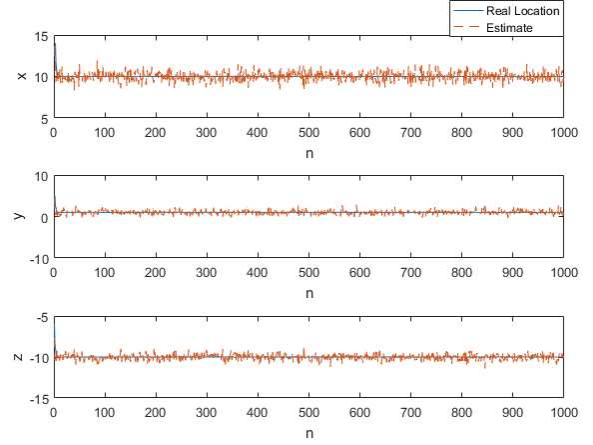


Fig. 1. Location tracking result for scenario 1.

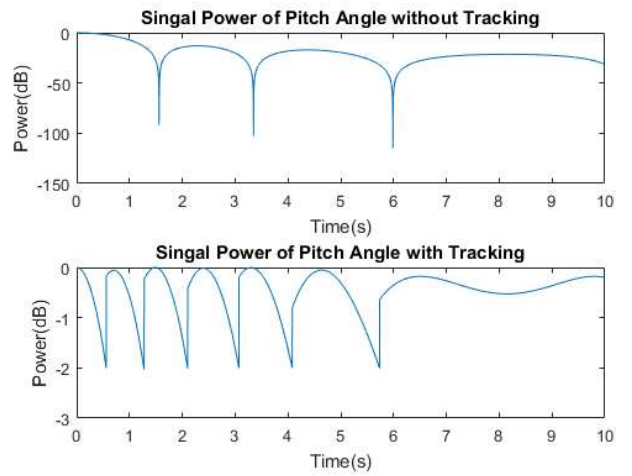


Fig. 2. Signal power with and without tracking of the pitch angle for scenario 1.

provides continuous high signal power during the process. A comparison of the three rotation angle simulation results shows that the number of adjusting beams for both roll and yaw rotations is much more than that of pitch rotation.

For the second scenario, the STD of the state vector is set to be  $1m/100T_t$  in x, y and z directions, respectively. The tracking update time is  $100T_t$ . The operation time is  $16.73s$  with a rotation speed of  $0.1^\circ/100T_t$ . Apart from that, the other settings are unchanged from scenario 1. Fig. 5 is the location tracking result for scenario 2 with an RMSE of 0.6055m. Compared with scenario 1, in Figs. 6-8, there are more variations caused by displacements of the UN in the received signal power, which are all above -3dB (half power) for the proposed tracking method, much higher than the case without tracking.

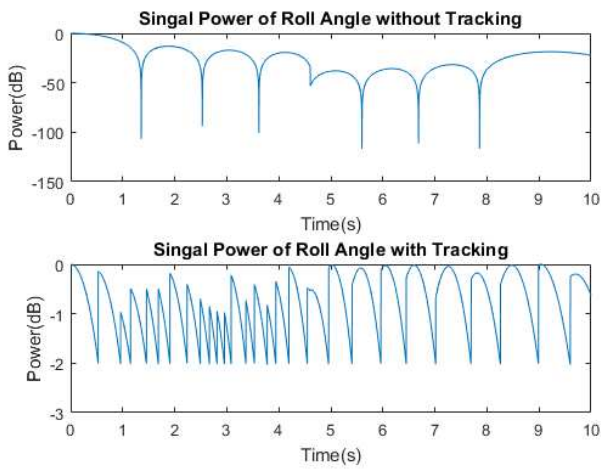


Fig. 3. Signal power with and without tracking of the roll angle for scenario 1.

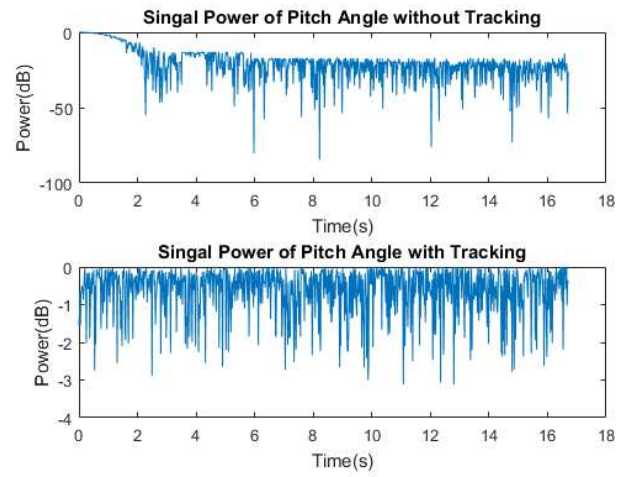


Fig. 6. Signal power with and without tracking of the pitch angle for scenario 2.

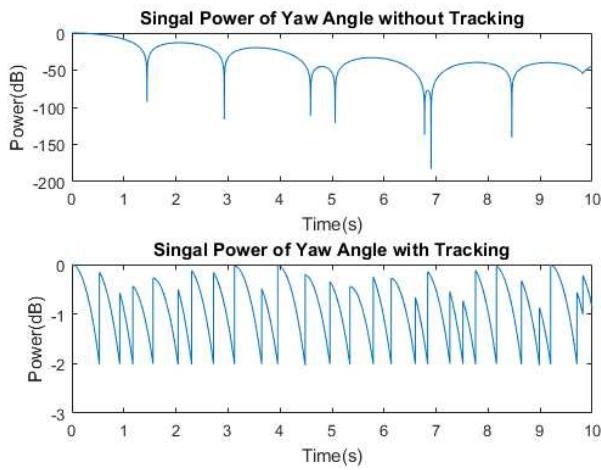


Fig. 4. Signal power with and without tracking of the yaw angle for scenario 1.

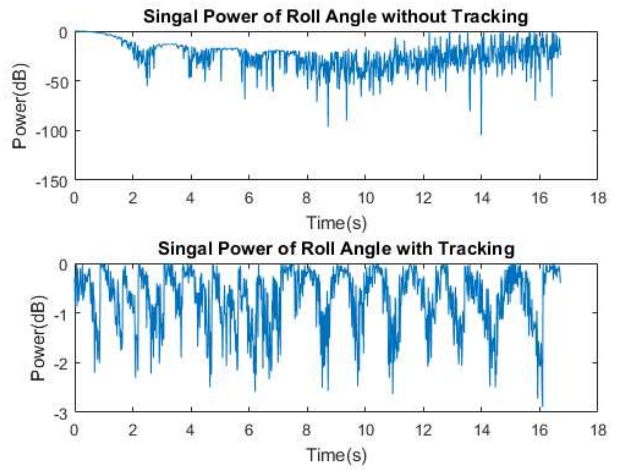


Fig. 7. Signal power with and without tracking of the roll angle for scenario 2.

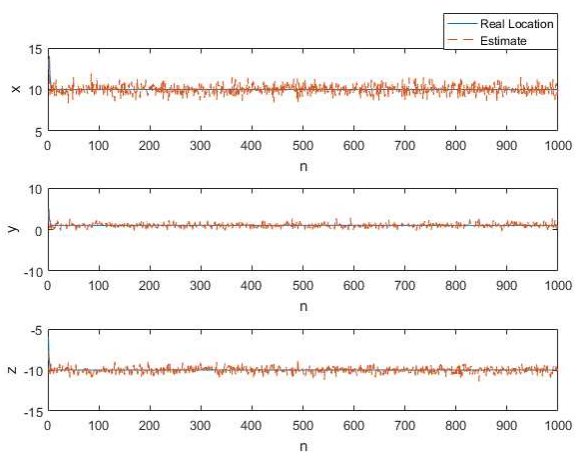


Fig. 5. Localazation tracking result in Scenario 2.

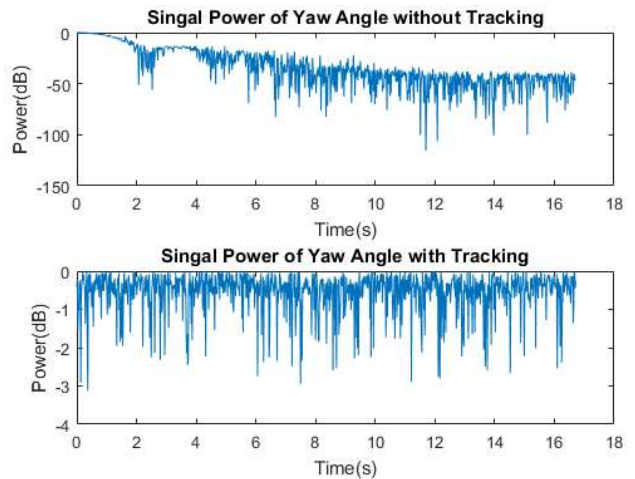


Fig. 8. Signal power with and without tracking of the yaw angle for scenario 2.

#### IV. CONCLUSION

A 3-D beam tracking method has been proposed for millimeter wave communication in the 5G ultra dense network scenario. It is based on measurements of the embedded MEMS sensors of the smart phone with extended Kalman filtering incorporating positioning methods for location tracking of the UN. It has been demonstrated that the proposed method for 3-D beam tracking can tackle the challenge posed by the UN's self-rotation to maintain the required beam alignment between AN and UN. Moreover, with the aid of location tracking, in a more complicated scenario, of which UN's displacement is also included, the proposed method has also worked effectively. In our future work, we will consider the scenario with significant movement of the UN across several ANs' coverage areas.

#### REFERENCE

- [1] Huawei. "5G: A technology vision (white paper)", 2013. Available: <http://www.huawei.com/5gwhitepaper/>.
- [2] D. Dardari, P. Closas, and Petar M. Djurić. Indoor tracking: Theory, methods, and technologies. *IEEE Transactions on Vehicular Technology*, 64(4):1263–1278, Apr. 2015.
- [3] J. Medbo, I. Siomina, A. Kangas, and J. Furuskog. Propagation channel impact on LTE positioning accuracy: A study based on real measurements of observed time difference of arrival. In *IEEE 20th International Symposium on Personal, Indoor and Mobile Radio Communications*, volume 4, 2009.
- [4] H. Liu, Y. Gan, J. Yang, S. Sidhom, Y. Wang, Y. Chen, and F. Ye. Push the limit of wifi based localization for smartphones. In *Proceedings of the 18th Annual International Conference on Mobile Computing and Networking*, volume 11, pages 305–316. ACM, 2012.
- [5] J. Werner, M. Costa, A. Hakkarainen, K. Leppanen, and M. Valkama. Joint user node positioning and clock offset estimation in 5G ultra-dense networks. In *IEEE Global Communications Conference (GLOBECOM)*, pages 1–7. IEEE, 2015.
- [6] J. Werner, J. Wang, A. Hakkarainen, D. Cabric, and M. Valkama. Performance and cramer–rao bounds for DoA/RSS estimation and transmitter localization using sectorized antennas. *IEEE Transactions on Vehicular Technology*, 65(5):3255–3270, 2016.
- [7] X. Cheng, D. Zhu, S. Zhang, and P. He. Tracking positioning algorithm for direction of arrival based on direction lock loop. *Future Internet*, 7(3):214–2242, 2015.
- [8] M. Giordani, M. Mezzavilla, A. Dhananjay, S. Rangan, and M. Zorzi. Channel dynamics and SNR tracking in millimeter wave cellular systems. (8), Apr. 2016.
- [9] M. Park and Helen K. Pan. Effect of device mobility and phased array antennas on 60 Ghz wireless networks. In *Proceedings of the ACM International Workshop on mmWave Communications: From Circuits to Networks*, pages 51–56. ACM, 2010.
- [10] Y. Inoue, Y. Kishiyama, Y. Okumura, J. Kepler, and M. Cudak. Experimental evaluation of downlink transmission and beam tracking performance for 5G mmW radio access in indoor shielded environment. In *Personal, Indoor, and Mobile Radio Communications (PIMRC), IEEE 26th Annual International Symposium on*, pages 862–866. IEEE, 2015.
- [11] D. Shim, C. Yang, J. Kim, J. Han, and Y. Cho. Application of motion sensors for beam-tracking of mobile stations in mmwave communication systems. *Sensors*, 14(10):19622–19638, 2014.
- [12] D. Simon. *Optimal State Estimation: Kalman, H Infinity, and Nonlinear Approaches*. Hoboken, N.J: Wiley-Interscience, 1st edition, Jun 2006.
- [13] R.G. Valenti, I. Dryanovski, and J. Xiao. Keeping a good attitude: A quaternion-based orientation filter for imus and margs. *Sensors*, 15(8):19302–19330, 2015.
- [14] D. Harville. Extension of the gauss-markov theorem to include the estimation of random effects. *The Annals of Statistics*, pages 384–395, 1976.
- [15] Gregory G. Slabaugh. Computing euler angles from a rotation matrix. *Retrieved on August*, 6(2000):39–63, 1999.
- [16] M. D. Jiang, Y. Li, and W. Liu. Properties of a general quaternion-valued gradient operator and its application to signal processing. *Frontiers of Information Technology & Electronic Engineering*, 17:83–95, February 2016.
- [17] W. Liu and S. Weiss. *Wideband Beamforming: Concepts and Techniques*. John Wiley & Sons, Chichester, UK, 2010.
- [18] M. Longbrake. True time-delay beamsteering for radar. In *Aerospace and Electronics Conference (NAECON), IEEE National*, pages 246–249. IEEE, 2012.
- [19] P. Kela, M. Costa, J. Salmi, K. Leppanen, J. Turkka, T. Hiltunen, and M. Hronec. A novel radio frame structure for 5G dense outdoor radio access networks. In *IEEE 81st Vehicular Technology Conference (VTC Spring)*, pages 1–6. IEEE, 2015.